Molecular-dynamics study of second sound

T. Schneider and E. Stoll
IBM Zurich Research Laboratory, 8803 Rüschlikon ZH, Switzerland
(Received 10 April 1978)

Using a molecular-dynamics technique simulating a canonical ensemble with nearly conserved energy, we studied the occurrence and some properties of second sound in terms of the calculated spectral densities. We considered two models: model I exhibiting a ferrodistortive phase, where displacement and energy fluctuations are coupled and third-order anharmonicity is dominant at low temperatures, and model II, where there is no ordered phase, and quartic anharmonicity is present only. Both models exhibit an optical-phonon branch only. Our molecular-dynamics technique makes it possible to study second sound and its damping in terms of a resonance in the appropriate spectral densities. The results confirm the existence of a temperature window, where well-defined second sound occurs. They also suggest that second sound might be a rather usual low-temperature phenomenon, provided the crystal is sufficiently clean.

I. INTRODUCTION AND SUMMARY

The phenomena connected with the transport of heat in an insulating solid can usually be understood in terms of diffusive heat conduction. An exceptional type of behavior has been observed, however, in a few substances in a narrow temperature window: second sound, a wavelike propagation of heat. Second sound was first observed by Ackermann *et al.*[1] in solid ^{4}He. Subsequently, further successful heat-pulse experiments on ^{3}He, NaF, and Bi were reported.[2-4] Recently, Pohl and Irniger[5] succeeded in probing second sound more directly by means of forced thermal light scattering.

The molecular-dynamics technique has also been applied, aimed at investigating linear[6] and nonlinear[7,8] heat-pulse propagation. We used a molecular-dynamics technique, simulating a canonical ensemble with nearly conserved energy, so that second sound led to a resonance in the appropriate spectral densities.[8] Here, we extend these results and relate them to theoretical treatments.

In the numerical approach, the system is simply defined by its Hamiltonian. Accordingly, if not built in, there are no impurities, dislocations, which usually suppress the occurrence of second sound. However, there are also limitations: finite systems can be treated only, the time interval over which the dynamics can be followed is rather limited, and the results are valid only within the framework of classical mechanics. The latter limitation is particularly important, as second sound is a low-temperature phenomenon. Nevertheless, the numerical results may be related to the theoretical treatments because they do have a well-defined classical limit. In view of this, the molecular-dynamics technique appears to be a valuable complementary tool to test the validity and limitations of the theoretical treatments on second sound.

As far as the state of the art of the theory is concerned, we refer to the recent reviews of Enz[9] and Beck.[10]

In this paper, we study two model systems. Common features are that the displacement vector is a scalar and that the particles can displace only with respect to a rigid reference lattice. As a consequence, there is an optical phonon branch only. It belongs to the family of models which has been used with remarkable success to elucidate the critical properties associated with ferro and antiferrodistortive phase transitions.[11] Model I does exhibit a ferrodistortive phase at low temperatures so that displacement and energy fluctuations are coupled below T_c. Owing to this feature, second sound is expected to appear in both the displacement and energy spectral density. Moreover, third-order anharmonicity is dominant at low temperature. Model II does not exhibit an ordered phase, and fourth-order anharmonicity is present only. Accordingly, displacement and energy fluctuations are not coupled. This choice of the models allows the study of second sound under quite different conditions, namely, presence or absence of a coupling between energy and displacement fluctuations and third- or fourth-order anharmonicity. Without particularly chosen model parameters, well-defined second sound appears in both models in a temperature window. This result suggests that second sound might be a rather usual phenomenon in sufficiently ideal systems.

Section II is devoted to the definition of the models, the conservation laws, a short sketch of the resolvent representation of Green's function, the perturbation treatment of the anharmonic terms, a four-variable theory treatment of the coupled dynamic variables, and to a sketch of the hydrodynamic approach. These results can, quite quantitatively, account for the molecular-dynamics results presented in Sec. III. Here, we also sketch

our molecular-dynamics technique, by means of which the displacement and energy spectral densities have been calculated. In model I, where energy and displacement fluctuations are coupled, a well-defined second-sound resonance appearing in a temperature window occurs in both the displacement and energy spectral densities. The displacement spectral density is dominated by the phonon resonance, whereas the strength of the second-sound peak is weak. In the energy spectral density, this behavior is reversed. These results agree quite well with the four-variable theory, which takes the coupling between displacement and energy fluctuations into account. Comparison with the form of the energy spectral density predicted by the hydrodynamic approach leads to quite good agreement, and confirms the existence of a temperature window where well-defined second sound occurs. For the temperature dependence of the relaxation times for normal and umklapp processes entering the hydrodynamic approach, we invoke the results obtained from anharmonic perturbation theory. In model I, third-order anharmonicity is dominant at low temperatures.

In model II, where only fourth-order anharmonicity is present, we also find quite good agreement between the numerical results and the form of the spectral density predicted by the hydrodynamic approach. In this model, well-defined second sound is again confined to a temperature window. Our results also reveal that well-defined second sound is not restricted to very small wave vectors.

II. MODEL SYSTEMS AND THEORETICAL DESCRIPTION

In this section, we define the model, its continuum limit, the dynamic variables of interest, and the relevant conservation laws. Moreover, we shall outline the resolvent representation of Green's functions[12,13] to describe the excitation spectrum, including second sound, and will briefly review the main results as obtained from the Peierls' equation and hydrodynamic equations.[10,14]

A. Model, dynamic variables, and conservation laws

The Hamiltonian of the ferrodistortive model is

$$\mathcal{H}=\sum_l \frac{M\dot{X}_l^2}{2}+\frac{A-12C}{2}\sum_l X_l^2+\frac{B}{4}\sum_l X_l^4 + \frac{C}{2}\sum_{\langle l,l'\rangle}(X_l-X_{l'})^2 . \tag{1}$$

l labels the particle with mass M in the lth unit cell; $M\dot{X}_l$ and X_l are momentum and displacement with respect to a rigid cubic primitive reference lattice. The last term in Eq. (1) includes nearest-neighbor interactions only; M, A, B, and C are the model parameters chosen as, for model I,

$$A=-1,\quad B=\tfrac{1}{3},\quad C=\tfrac{1}{6},\quad M=1 \tag{2}$$

and for model II,

$$A=3,\quad B=\tfrac{1}{3},\quad C=\tfrac{1}{6},\quad M=1 . \tag{3}$$

Here, we have adopted the same units as in Ref. 15. The order parameter at zero temperature ($T=0$) is, within the framework of classical mechanics, given by

$$X_l^2=(12C-A)/B , \tag{4}$$

provided that

$$12C-A\geq 0 . \tag{5}$$

For $12C-A<0$, there is no ordered phase at $T=0$. More generally, it has been shown[16] that for $12C-A>0$, the system will undergo a second-order phase transition at some $T=T_c>0$. Accordingly, model I [Eq. (2)], which has been studied in Ref. 8, exhibits a ferrodistortive second-order phase transition, while model II [Eq. (3)] is disordered at all temperatures.

To describe the static and dynamic properties of the system, we next consider the following variables:

$$\dot{X}(\vec{q})=\frac{1}{\sqrt{N}}\sum_l \dot{X}_l e^{i\vec{q}\cdot\vec{R}_l} , \tag{6}$$

$$X(\vec{q})=\frac{1}{\sqrt{N}}\sum_l \delta X_l e^{i\vec{q}\cdot\vec{R}_l} , \tag{7}$$

$$\mathcal{H}(\vec{q})=\frac{1}{\sqrt{N}}\sum_l \delta\mathcal{H}_l e^{i\vec{q}\cdot\vec{R}_l} , \tag{8}$$

where

$$\delta X_l=X_l-\langle X_l\rangle , \tag{9}$$

$$\delta\mathcal{H}_l=\mathcal{H}_l-\langle\mathcal{H}_l\rangle , \tag{10}$$

$$\mathcal{H}_l=\tfrac{1}{2}M\dot{X}_l^2+\tfrac{1}{2}AX_l^2+\tfrac{1}{4}BX_l^4-C\sum_{l'}X_lX_{l'} . \tag{11}$$

These variables describe momentum, displacement, and energy fluctuations, respectively, of wave vector $\vec{q}$. The vectors $\vec{R}_l$ define the direct rigid reference lattice.

From Eqs. (6) and (8), we find for the rate of change of the momentum and energy fluctuations

$$\ddot{X}(\vec{q})=-\frac{1}{\sqrt{N}}\sum_l e^{i\vec{q}\cdot\vec{R}_l}\frac{1}{M}\left[(A-12C)X_l+BX_l^3 + 2C\sum_{l'}(X_l-X_{l'})\right] , \tag{12}$$

$$\dot{\mathcal{K}}(\vec{q}) = 2C\frac{1}{N}\sum_{\vec{q}'}[X(\vec{q}-\vec{q}')\dot{X}(\vec{q}') - \dot{X}(\vec{q}-\vec{q}')X(\vec{q}')]F(\vec{q}') + 2C\langle X\rangle[3-F(\vec{q})]\dot{X}(\vec{q}), \tag{13}$$

where

$$F(\vec{q}) = \cos q_x a + \cos q_y a + \cos q_z a, \tag{14}$$

a being the lattice constant of the rigid cubic primitive reference lattice. $\mathcal{K}(\vec{q}=0,t)$ is seen to vanish, so that energy is conserved as it should be for a Hamiltonian system. Momentum is not conserved in the system considered here because $\ddot{X}(\vec{q}=0,t) \neq 0$. Consequently, among the variables considered here, energy is the only conserved one. At sufficiently low temperatures, however, where umklapp processes are rare, one expects the quasimomentum to become an additional, but only nearly conserved variable. To derive a formal expression of this nearly conserved quantity, we next consider the continuum approximation of the model defined by Hamiltonian (1). The associated Lagrangian reads

$$\mathfrak{L} = \int d^3X\, L, \tag{15}$$

where

$$L = T - V, \tag{16}$$

$$T = \tfrac{1}{2}M\dot{f}^2(\vec{X},t), \tag{17}$$

$$V = \tfrac{1}{2}(A-12C)f^2 + \tfrac{1}{4}Bf^4 + Ca^2(\nabla f)^2, \tag{18}$$

L being the Lagrangian density of the displacement field f. The corresponding Lagrange-Euler equation is

$$\nabla\left(\frac{\partial L}{\partial \nabla f}\right) + \frac{\partial}{\partial t}\frac{\partial L}{\partial \dot{f}} - \frac{\partial L}{\partial f} = 0. \tag{19}$$

Inspection reveals that not only the energy density

$$H = T + V, \tag{20}$$

but also the field-momentum density

$$\vec{Q} = -M\dot{f}\nabla f \tag{21}$$

are conserved. The corresponding conservation laws read

$$\frac{\partial H}{\partial t} = \nabla\cdot\vec{J}_H = 2Ca^2(\nabla f\cdot\nabla\dot{f} + \Delta f\dot{f}), \tag{22}$$

where

$$\vec{J}_H = 2Ca^2\dot{f}\nabla f \tag{23}$$

is the energy current, and

$$\frac{\partial\vec{Q}}{\partial t} + \nabla J_Q = 0, \tag{24}$$

where the field-momentum current is given by

$$J_Q = L + 2Ca^2(\nabla f)^2. \tag{25}$$

This section has revealed that energy is an exactly conserved variable, and field momentum a nearly conserved variable. The field momentum is nearly conserved only, because its derivation *relies* on the continuum approximation, where umklapp processes are neglected. To illustrate the importance of conserved variables in a description of the dynamic properties, we consider the correlation function

$$\langle\mathcal{K}(-\vec{q},t)\mathcal{K}(\vec{q},0)\rangle = \langle\mathcal{K}(-\vec{q},0)\mathcal{K}(\vec{q},0)\rangle - \tfrac{1}{2}t^2\langle\dot{\mathcal{K}}(-\vec{q},0)\dot{\mathcal{K}}(\vec{q},0)\rangle + \tfrac{1}{4}t^4\langle\ddot{\mathcal{K}}(-\vec{q},0)\ddot{\mathcal{K}}(\vec{q},0)\rangle - \cdots + \cdots. \tag{26}$$

Energy conservation [Eq. (13)] implies that in the limit $\vec{q}\to\vec{0}$, the t-dependent terms vanish. Hence,

$$\lim_{\vec{q}\to\vec{0}} S_{\mathcal{K}\mathcal{K}}(\vec{q},\omega) = \lim_{\vec{q}\to\vec{0}}\int_{-\infty}^{+\infty} dt\, e^{-i\omega t}\langle\mathcal{K}(-\vec{q},t)\mathcal{K}(\vec{q},0)\rangle = \langle\mathcal{K}(\vec{0},0)\mathcal{K}(\vec{0},0)\rangle\delta(\omega), \tag{27}$$

exhibiting a singularity at zero frequency. In the present case, where energy is conserved, this singularity signals the occurrence of a hydrodynamic mode at finite $\vec{q}$, namely, heat diffusion, representing overdamped second sound. Propagating second sound can be expected only if the field momentum is also nearly conserved. The appearance of these hydrodynamic modes is not restricted to Green's functions of the conserved variables, but may occur in those Green's functions where the associated dynamic variable is coupled to the conserved ones.

B. Green's-function approach

To describe the excitation spectrum, we next adopt the resolvant representation of the relevant Green's functions. Without going into details of this representation, we sketch below the structure of the theory and apply it to the present model. For details, we refer to Refs. 12 and 13.

We consider the retarded Green's function

$$G^{\dagger}_{AA}(t) = -i\Theta(t)\langle[A^{\dagger}(t),A]\rangle. \tag{28}$$

Using the identity

$$-i\langle[A^{\dagger}(t),A]\rangle = \int_0^{\beta} d\lambda\,\langle e^{\lambda\mathcal{K}}\dot{A}^{\dagger}(t)e^{-\lambda\mathcal{K}}A(0)\rangle \equiv \dot{A}/A, \tag{29}$$

Eq. (28) may be rewritten

$$G^{\dagger}_{AA}(t) = \dot{A}(t)/A, \quad t>0, \tag{30}$$

or in the classical limit

$$G^{\dagger}_{AA}(t)=\beta\langle\dot{A}(t)/A\rangle, \quad t>0. \tag{31}$$

Introducing the Liouville operator

$$A(t)=e^{iLt}A(0), \tag{32}$$

we find

$$G^{\dagger}_{AA}(z)=\beta\int_0^{\infty} e^{-zt}\langle\dot{A}(t)/A\rangle\,dt$$
$$=\beta\left(-\langle A/A\rangle+\langle A|\frac{z}{z+iL}|A\rangle\right). \tag{33}$$

With the aid of the projection operator

$$P=|A\rangle\frac{1}{\langle A/A\rangle}\langle A|, \quad Q=1-P, \tag{34}$$

one may rewrite Eq. (33) in the form

$$G^{\dagger}_{AA}(z)=-\beta\langle A/A\rangle[z\langle A/A\rangle+\langle\dot{A}/A\rangle+F_{AA}(z)]^{-1}$$
$$\times[\langle\dot{A}/A\rangle+F_{AA}(z)], \tag{35}$$

where

$$F_{AA}(z)=\langle\dot{A}|Q\frac{1}{z+iQLQ}Q|\dot{A}\rangle. \tag{36}$$

The extension of n dynamic variables, where Eq. (35) is an equation of the $n\times n$ Green's functions, is

$$G^{\dagger}(z)=-\beta a(za+\omega+F)^{-1}(\omega+F), \tag{37}$$

where

$$a_{ij}=\langle A_i/A_j\rangle, \tag{38}$$
$$\omega_{ij}=\langle\dot{A}_i/A_j\rangle, \tag{39}$$
$$F_{ij}=\langle\dot{A}_i|Q\frac{1}{z+iQLQ}Q|\dot{A}_j\rangle, \tag{40}$$
$$P=\sum_{i,j}|A_i\rangle(a^{-1})_{ij}\langle A_j|, \quad Q=1-P. \tag{41}$$

The advantage of considering a matrix of Green's function stems from the fact that the coupling of conserved variables may be taken into account from the outset. The various poles corresponding to different possible excitations are then obtained in a direct way without the complicated treatment of hydrodynamic singularities of other approaches.

C. Perturbation theory

In this subsection, we shall work out approximations for $G^{\dagger}_{XX}(z)$ and $G^{\dagger}_{\mathcal{H}\mathcal{H}}(z)$ by treating the anharmonic terms as perturbations. On this basis, it becomes possible to discuss the damping and frequency shift of the phonons, and also to identify the hydrodynamic singularities.

To formulate a perturbation theory within the framework of a one-variable theory, we note that according to Eq. (33),

$$G^{\dagger}_{AA}(z)-G^{\dagger}_{AA}(z=0)=\beta\left\langle A\frac{z}{z+iL}A\right\rangle$$
$$=\beta zS_{AA}(z). \tag{42}$$

A perturbation theory may be obtained by setting

$$L=L_0+L_1, \tag{43}$$

where

$$-iL_0=\sum_l\frac{\partial\mathcal{H}_0}{\partial P_l}\frac{\partial}{\partial X_l}-\frac{\partial\mathcal{H}_0}{\partial X_l}\frac{\partial}{\partial P_l}, \tag{44}$$
$$-iL_1=\sum_l\frac{\partial\mathcal{H}_1}{\partial P_l}\frac{\partial}{\partial X_l}-\frac{\partial\mathcal{H}_1}{\partial X_l}\frac{\partial}{\partial P_l}, \tag{45}$$
$$P_l=M\dot{X}_l. \tag{46}$$

Using the identity

$$\frac{1}{A+B}=\frac{1}{A}-\frac{1}{A}B\frac{1}{A+B}, \tag{47}$$

we obtain for $S(z)$ the expansion

$$S_{AA}(z)=\left\langle A\frac{1}{z+iL_0}A\right\rangle-\left\langle A\frac{1}{z+iL_0}iL_1\frac{1}{z+iL_0}A\right\rangle$$
$$+\left\langle A\frac{1}{z+iL_0}iL_1\frac{1}{z+iL_0}iL_1\frac{1}{z+iL_0}A\right\rangle-+\cdots \tag{48}$$

which may be used to derive approximate expressions for the memory function $\tilde{\Sigma}(z)$ in the expression

$$G^{\dagger}_{AA}(z)=-\frac{1}{z^2+\omega_0^2+z\tilde{\Sigma}_{AA}(z)}. \tag{49}$$

Next we consider model II [Eq. (3)], which does not exhibit an ordered phase, and linearize the quartic term in lowest order to define $\mathcal{H}_0$. According to Eq. (1), $\mathcal{H}_0$ and $\mathcal{H}_1$ are then given by

$$\mathcal{H}_0=\sum_l\frac{P_l^2}{2M}+\frac{A-12C}{2}\sum_l X_l^2+\tfrac{3}{2}B\langle X_l^2\rangle\sum_l X_l^2$$
$$+\frac{C}{2}\sum_{l,l'}(X_l-X_{l'})^2, \tag{50}$$

$$\mathcal{H}_1=\frac{B}{4}\sum_l X_l^4-\tfrac{3}{2}B\langle X_l^2\rangle\sum_l X_l^2, \tag{51}$$

defining according to Eqs. (44) and (45), the decomposition of the Liouville operator. By evaluating the trace with respect to $\mathcal{H}_0$ and taking the first three terms of the expansion (48) into account, we find for ω_0^2 and the memory function Σ the expressions

$$M\omega_0^2=(A-12C)+3B\langle X^2\rangle+4C[3-F(\vec{q})] \tag{52}$$

and

$$\Sigma_{XX}(\vec{q},z)=\frac{3B^2(k_BT)^2}{8}\frac{1}{N^2}\sum_{\vec{q}_1\vec{q}_2\vec{q}_3}\Delta(\vec{q}_1+\vec{q}_2+\vec{q}_3+\vec{q})\frac{1}{\omega_0^2(\vec{q}_1)\omega_0^2(\vec{q}_2)\omega_0^2(\vec{q}_3)}\sum_{(\pm)}\left(\frac{1}{z+i[\pm\omega_0(\vec{q}_1)\pm\omega_0(\vec{q}_2)\pm\omega_0(\vec{q}_3)]}\right). \quad (53)$$

The crucial point in this context is, apart from T^2 dependence of the self-energy, that no singularity appears in the limit $\vec{q}\to 0, z\to 0$. This reveals that the approximate expression (54) is valid for all z at sufficiently low temperature because there is no coupling between the displacement fluctuations and energy fluctuations in this model.

The energy Green's function is expected, however, to exhibit such a singularity. This may be demonstrated by calculating $G^{\dagger}_{\mathcal{H}\mathcal{H}}(\vec{q},z)$ in zero order. The result is

$$G^{\dagger}_{\mathcal{H}\mathcal{H}}(\vec{q},z)-G^{\dagger}_{\mathcal{H}\mathcal{H}}(\vec{q},z=0)=\beta z S_{\mathcal{H}\mathcal{H}}(\vec{q},z), \quad (54)$$

where

$$S_{\mathcal{H}\mathcal{H}}(\vec{q},z)=\frac{(k_BT)^2}{16N}\sum_{\vec{q}'}\frac{1}{\omega_0^2(\vec{q}')\omega_0^2(\vec{q}-\vec{q}')}\times\Big\{[\omega_0(\vec{q}')-\omega_0(\vec{q}-\vec{q}')]^4\left(\frac{1}{z+i[\omega_0(\vec{q}')+\omega_0(\vec{q}-\vec{q}')]}+\frac{1}{z-i[\omega_0(\vec{q}')+\omega_0(\vec{q}-\vec{q}')]}\right)$$
$$+[\omega_0(\vec{q}')+\omega(\vec{q}-\vec{q}')]^4\left(\frac{1}{z+i[\omega_0(\vec{q}')-\omega_0(\vec{q}-\vec{q}')]}+\frac{1}{z-i[\omega_0(\vec{q}')-\omega_0(\vec{q}-\vec{q}')]}\right)\Big\} \quad (55)$$

which has a singularity at $\vec{q}\to 0, z\to 0$, expressing energy conservation and signaling the occurrence of a hydrodynamic mode, namely, heat diffusion or second sound in the interacting case. Clearly, this singularity will appear in all orders, because it simply expresses conservation of energy. It demonstrates, however, that for $G^{\dagger}_{\mathcal{H}\mathcal{H}}(\vec{q},z)$, a perturbation theory breaks down for small $\vec{q}$ and z, or in other words, that hydrodynamic modes cannot be obtained in terms of a perturbation expansion in powers of the anharmonic terms.

To treat model I [Eq. (2)], exhibiting a phase transition, it is useful, at least at low temperatures, to rewrite Hamiltonian (1) in terms of the order parameter $\langle X_l\rangle$ and the deviations from this mean value, where

$$X_l=\langle X_l\rangle+\delta X_l. \quad (56)$$

The result is

$$\mathcal{H}=\mathcal{H}_0+\mathcal{H}_1,$$
$$\mathcal{H}_0=\cdots+\sum_l\frac{P_l^2}{2M}+\frac{A-12C}{2}\sum_l\delta X_l^2$$
$$+\tfrac{3}{2}B\langle X^2\rangle\sum_l\delta X^2+\frac{C}{2}\sum_{l,l'}(\delta X_l-\delta X_{l'})^2, \quad (57)$$
$$\mathcal{H}_1=B\langle X\rangle\sum_l\delta X_l^3+\frac{B}{4}\sum_l\delta X_l^4-\tfrac{3}{2}B\langle\delta X_l^2\rangle\sum_l\delta X_l^2, \quad (58)$$

where we cited only those terms which enter the dynamics. The crucial difference, compared with model II [Eqs. (50) and (51)], is the occurrence of third-order anharmonicity in the ordered phase, in addition to the quartic term. Here, we treat the third-order term only. Evaluating L_0 and L_1 according to Eqs. (44) and (45), we find for the self-energy defined by Eqs. (42), (48), and (49),

$$\Sigma_{XX}(\vec{q},z)=\frac{9\langle X\rangle^2B^2k_BT}{2}\sum_{\vec{q}'}\frac{1}{\omega_0^2(\vec{q}')\omega_0^2(\vec{q}-\vec{q}')}\left(\frac{1}{z+i[\omega_0(\vec{q}')-\omega_0(\vec{q}-\vec{q}')]}+\frac{1}{z-i[\omega_0(\vec{q}')-\omega(\vec{q}-\vec{q}')]}\right.$$
$$\left.+\frac{1}{z+i[\omega_0(\vec{q}')+\omega_0(\vec{q}-\vec{q}')]}+\frac{1}{z-i[\omega_0(\vec{q}')+\omega_0(\vec{q}-\vec{q}')]}\right). \quad (59)$$

This memory function becomes singular in the limit $\vec{q} \to \vec{0}, z \to 0$, the same as the Laplace transform of the energy correlation [Eq. (55)]. This singularity illustrates the coupling between order parameter and energy fluctuation in the ordered phase. As a consequence, thermal diffusion or second sound will also appear in the displacement Green's function for $T < T_c$.

D. Four-variable theory

To account for second sound or thermal diffusion, at the outset one has to take into account the conserved and coupled variables. This is conveniently achieved in terms of a many-variable theory, without the complicated treatment of the singularities appearing in the limit $\vec{q} \to \vec{0}, z \to 0$. In model I [Eq. (2)], where below T_c order parameter and energy fluctuations couple, it appears appropriate to consider the order-parameter (displacement) fluctuations $X(\vec{q})$, the corresponding momentum $\dot{X}(\vec{q})$, the energy $\mathcal{H}(\vec{q})$, and the field momentum $\vec{Q}(\vec{q})$ as dynamic variables. Energy and field momentum are conserved variables [Eqs. (22) and (24)] and $X(\vec{q}), \dot{X}(\vec{q})$ are needed to describe the phonons.

To simplify the discussion, we ignore the memory function matrix. Accordingly, we assume that second sound is a well-defined excitation. In this case, the Green's-function matrix is [Eq. (37)]

$$G^{\dagger}(z) = -\beta a(za + \omega)^{-1}\omega = -\beta(zE - \omega a^{-1})^{-1}\omega \tag{60}$$

with variables

$$X(\vec{q}),\ \mathcal{H}(\vec{q}),\ \dot{X}(\vec{q}),\ Q_1(\vec{q}),\ Q_2(\vec{q}),\ Q_3(\vec{q}). \tag{61}$$

For small wave vectors $\vec{q}$, the expressions for $\mathcal{H}(\vec{q})$ and $\vec{Q}(\vec{q})$ may be simplified by taking the Fourier transform of the corresponding expressions valid in the continuum approximation. From Eq. (21), we find

$$\vec{Q}(\vec{q}) = -i\frac{M}{\sqrt{N}}\sum_{\vec{q}'}\vec{q}'X(\vec{q}')\dot{X}(\vec{q}-\vec{q}'), \tag{62}$$

and from Eq. (22)

$$\mathcal{H}(\vec{q}) = -2Ca^2\frac{1}{\sqrt{N}}\sum_{\vec{q}'}\vec{q}\cdot\vec{q}'X(\vec{q}')X(\vec{q}-\vec{q}'). \tag{63}$$

Here, we have replaced the field fluctuations $f(\vec{q})$ by the displacement fluctuations $X(\vec{q})$. By choosing $\vec{q} = (q_1, 0, 0)$, there is no longer a coupling between the first four variables and the second and third components of the field momentum. Consequently, we have to consider only the first four variables in Eq. (61). The matrices a and ω are then given by

$$a = \begin{bmatrix} a_{11} & a_{12} & 0 & 0 \\ a_{21} & a_{22} & 0 & 0 \\ 0 & 0 & a_{33} & 0 \\ 0 & 0 & 0 & a_{44} \end{bmatrix}, \tag{64}$$

$$\omega = \begin{bmatrix} 0 & 0 & \omega_{13} & 0 \\ 0 & 0 & 0 & \omega_{24} \\ \omega_{31} & 0 & 0 & 0 \\ 0 & \omega_{42} & 0 & 0 \end{bmatrix}, \tag{65}$$

where

$$\begin{aligned} a_{11} &= \langle X(\vec{q}) | X(\vec{q})\rangle, \quad \omega_{13} = \langle \dot{X}(\vec{q}) | \dot{X}(\vec{q})\rangle = -\omega_{31} = a_{33}; \\ a_{12} &= \langle X(\vec{q}) | \mathcal{H}(\vec{q})\rangle, \quad \omega_{24} = \langle \mathcal{H}(\vec{q}) | Q_1(\vec{q})\rangle = -\omega_{42}; \\ a_{22} &= \langle \mathcal{H}(\vec{q}) | \mathcal{H}(\vec{q})\rangle, \quad a_{44} = \langle Q_1(\vec{q}) | Q_1(\vec{q})\rangle; \\ a_{33} &= \langle \dot{X}(\vec{q}) | \dot{X}(\vec{q})\rangle. \end{aligned} \tag{66}$$

From Eqs. (62) and (63), we find

$$a_{44} = \langle Q_1(q_1) | Q_1(q_1)\rangle = \frac{k_B T}{N}\ \frac{1}{N}\sum_{\vec{q}'} q_1'^2 \langle |X(\vec{q}')|^2\rangle, \tag{67}$$

$$\omega_{24} = \langle \dot{\mathcal{H}}(q_1) | Q_1(q_1)\rangle = iq_1 2Ca^2\frac{1}{N}\sum_{\vec{q}'} q_1'^2 \langle X(\vec{q}')|^2\rangle k_B T. \tag{68}$$

Moreover, a_{33} is given by

$$a_{33} = \langle \dot{X}(q_1) | \dot{X}(q_1)\rangle = k_B T/M. \tag{69}$$

The relevant Green's functions can now be calculated by matrix algebra. This leads to the following expressions:

$$G_{11}^{\dagger} = G_{XX}^{\dagger} = -\beta a_{11}\omega_T^2\ \frac{z^2 + b\omega_S^2}{(z^2 + b\omega_S^2)(z^2 + b\omega_T^2) - \omega_S^2\omega_T^2 b^2(1 - 1/b)}, \tag{70}$$

$$G_{22}^{\dagger} = G_{\mathcal{H}\mathcal{H}}^{\dagger} = -\beta a_{22}\omega_S^2\ \frac{z^2 + b\omega_T^2}{(z^2 + b\omega_S^2)(z^2 + b\omega_T^2) - \omega_S^2\omega_T^2 b^2(1 - 1/b)}, \tag{71}$$

where

$$\omega_T^2 = \frac{a_{33}}{a_{11}} = \frac{k_B T}{M\langle |X(q_1)|^2\rangle}, \tag{72}$$

$$b = \frac{a_{11}a_{22}}{a_{11}a_{22} - a_{12}a_{21}}, \tag{73}$$

$$\omega_S^2 = \frac{|\omega_{24}|^2}{a_{44}a_{22}}. \tag{74}$$

The poles are given by

$$2z_{\pm}^2 = -b(\omega_S^2 + \omega_T^2) \pm [b^2(\omega_S^2 - \omega_T^2)^2 + 4\omega_S^2\omega_T^2 b^2(1 - 1/b)]^{1/2}, \tag{75}$$

where z_+ describes the phonon branch and z_- second sound. The important feature is that second sound will appear in both $G^{\dagger}_{XX}$ and $G^{\dagger}_{\mathcal{H}\mathcal{H}}$ provided the coupling between order parameter and energy fluctuations, a_{12}, does not vanish. In fact, for $T > T_c$, where $a_{12} = 0$ in model I, or in model II, where an ordered phase does not occur, the Green's functions (70) and (71) reduce to

$$G^{\dagger}_{XX} = -\beta a_{11}\omega_T^2/(z^2 + \omega_T^2), \tag{76}$$

$$G^{\dagger}_{\mathcal{H}\mathcal{H}} = -\beta a_{22}\omega_S^2/(z^2 + \omega_S^2). \tag{77}$$

In this case, the second-sound frequency is simply given by ω_S [Eq. (74)]. To compare the second frequencies z_- and ω_S with other estimates, it is useful to calculate the associated velocity. For this purpose, we need to estimate the leading q dependence of the terms entering Eq. (75) at low temperatures, where second sound is expected to occur. Here, ω_T^2 is approximately given by Eq. (52). In addition,

$$a_{12} = \langle X(\vec{0}) | \mathcal{H}(\vec{0}) \rangle = k_B T^2 \frac{d\langle X \rangle}{dT},$$
$$a_{22} = \langle \mathcal{H}(\vec{0}) | \mathcal{H}(\vec{0}) \rangle = k_B T^2 \frac{d\langle \mathcal{H} \rangle}{dT} \approx (k_B T)^2, \tag{78}$$

and according to Eqs. (67), (68), and (74),

$$\omega_S^2 = \tfrac{1}{3}\vec{q}_1^2 \left(\frac{1}{N}\sum_{\vec{q}'} \vec{q}' \frac{\partial\omega_0}{\partial\vec{q}'} \frac{1}{\omega_0(\vec{q}')}\right)^2 \Big/ \left(\frac{1}{N}\sum_{\vec{q}'} \vec{q}'^2 \frac{1}{\omega_0^2(\vec{q}')}\right)$$
$$= q_1^2 4Ca^2 \frac{1}{N}\sum_{\vec{q}'} q_1'^2 \frac{1}{\omega_0^2(\vec{q}')}, \tag{79}$$

where the phonon frequency ω_0 is given by Eq. (52). Using the above leading q dependence, we find for the second-sound velocity,

$$-\lim_{q\to 0} \frac{z_-^2}{q^2} = C_{ss}^2$$
$$= \frac{1}{3}\left[\left(\frac{1}{N}\sum_{\vec{q}'} \vec{q}' \frac{\partial\omega_0}{\partial\vec{q}'} \frac{1}{\omega_0^2(\vec{q}')}\right)^2 \Big/ \left(\frac{1}{N}\sum_{\vec{q}'} \vec{q}'^2 \frac{1}{\omega_0^2(\vec{q}')}\right)\right] b(0)$$
$$= b(0) \lim_{q\to 0} \frac{\omega_S^2}{q^2}. \tag{80}$$

In model II, where a_{12} [Eq. (73)] vanishes, $b(0) = 1$. If an ordered phase is present, however, $b(0)$ is slightly larger than 1, giving rise to a shift of the second-sound velocity due to the coupling between order parameter and energy fluctuations. To estimate this shift, we substitute the relevant expressions (78) into Eq. (73). The result is

$$b(0) = \left[1 - \frac{T}{k_B} M\omega_0^2(0)\left(\frac{d\langle X \rangle}{dT}\right)^2\right]^{-1}. \tag{81}$$

For $T \to 0$, the leading temperature dependence of the order parameter is given by

$$\langle X \rangle = \left(\frac{12C - A}{B}\right)^{1/2} - \tfrac{3}{4} k_B T \frac{B^{1/2}}{(12C - A)^{3/2}}, \tag{82}$$

so that

$$\frac{d\langle X \rangle}{dT} = -\tfrac{3}{4} k_B \frac{B^{1/2}}{(12C - A)^{3/2}} \tag{83}$$

and, according to Eq. (81),

$$b(0) = \left(1 - \frac{9}{4} \frac{Bk_B T M\omega_0^2(0)}{(12C - A)^3}\right)^{-1}. \tag{84}$$

For model I [Eq. (2)], where $B = \frac{1}{3}$, $12C - A = 3$, and at low T [Eq. (52)] $M\omega_0^2(0) \approx 6$, expression (84) finally reduces at low temperatures to

$$b(0) = (1 - \tfrac{1}{6} k_B T)^{-1}. \tag{85}$$

Accordingly, the shift of the second-sound velocity or frequency will be small for $k_B T \ll 6$.

The identification of z_- or ω_S with the second-sound frequency becomes more convincing by noting that expression (75) agrees with the formula derived by Kwok,[17] using the Peierls-Boltzmann equation and the conservation of energy and quasimomentum. It is interesting to note, however, that expression (75) for the second-sound frequency also agrees in the continuum appproximation with our previous estimate,[8]

$$\omega_S^2 = \frac{\langle \dot{\mathcal{H}}(q_1) | \dot{\mathcal{H}}(q_1) \rangle}{\langle \mathcal{H}(q_1) | \mathcal{H}(q_1) \rangle} \approx q_1^2 4Ca^2 \frac{1}{N}\sum_{\vec{q}'} q_1'^2 \frac{1}{\omega_0^2(\vec{q}')}, \tag{86}$$

where $\dot{\mathcal{H}}(q_1)$ was considered as the fourth dynamic variable, instead of the field momentum $\vec{Q}$.

The Green's functions (70) and (71) have two

pairs of poles, one corresponding to the phonon branch and the other one representing propagating second sound. If order-parameter and energy fluctuations are uncoupled, however, the second-sound pole appears only in $G_{\mathcal{E}\mathcal{E}}$ [Eq. (77)]. Accordingly, the relative weight of the poles in $G_{\mathcal{E}\mathcal{E}}$ and G_{XX}, respectively, will depend on this coupling, measured by b [Eq. (85)]. The weight of the poles is given by the residue

$$R^{\pm}_{AA} = (z - z_{\pm}) G^{\pm}_{AA}(z)\big|_{z=z_{\pm}} . \tag{87}$$

From Eqs. (70), (71), and (75), we find for the ratio of the residues

$$R^{-}_{XX}/R^{+}_{XX} = (\omega_S/\omega_T)[1 - 1/b(0)] , \tag{88}$$

$$R^{+}_{\mathcal{E}\mathcal{E}}/R^{-}_{\mathcal{E}\mathcal{E}} = (\omega_S/\omega_T)^3[1 - 1/b(0)] . \tag{89}$$

Because $\omega_T \gg \omega_S$ and $1 - 1/b \ll 1$ [Eq. (85)], the residue of the second-sound peak is rather weak in G_{XX} and vanishes for $b = 1$. Hence, the phonon pole dominates. This behavior is reversed in $G^{\dagger}_{\mathcal{E}\mathcal{E}}$.

Owing to the neglect of the memory-function matrix in Eq. (60), we assumed that second sound and the phonons are extremely well-defined excitations. According to Sec. II C, this assumption is certainly valid for the phonons, provided the temperature is sufficiently low. Second sound, however, is a more delicate phenomenon,[9,10,18] because it is expected to occur only in a temperature window. At the upper limit, it becomes overdamped due to umklapp processes, and goes over to the thermal diffusion mode. At the lower limit, there are no longer sufficient phonon collisions to maintain local thermal equilibrium. Consequently, a full discussion of second sound and heat diffusion would require an evaluation of the memory-function matrix to estimate the damping. At present, we postpone this work and rely on the hydrodynamic approach to include damping on a phenomenological basis.

E. Hydrodynamic approach

In the hydrodynamic approach, it is assumed that the system can be described by a function $f(\vec{q}, \vec{r}, t)$, being the distribution of phonon wave packets of wave vector $\vec{q}$ and position $\vec{r}$. Its time evolution is governed by the Boltzmann-Peierls equation

$$\frac{\partial f}{\partial t} + \vec{V}_q \frac{\partial f}{\partial \vec{r}} = C[f], \tag{90}$$

where

$$\vec{V}(\vec{q}) = \frac{\partial \omega}{\partial \vec{q}} \tag{91}$$

denotes the group velocity. The collision operator describes the scattering processes between the phonons. The energy and quasimomentum density are defined by

$$E(\vec{r}, t) = \sum_{\vec{q}} \omega(\vec{q}) f(\vec{q}, \vec{r}, t) ,$$
$$Q_i(\vec{r}, t) = \sum_{\vec{q}} q_i f(\vec{q}, \vec{r}, t) . \tag{92}$$

Assuming umklapp processes are negligible, both energy and quasimomentum are conserved. One thus obtains the conservation laws

$$\dot{E}(\vec{r}, t) + \frac{\partial}{\partial r_i} J_{Ei}(\vec{r}, t) = 0 , \tag{93}$$

$$Q_i(\vec{r}, t) + \frac{\partial}{\partial r_j} J_{Qij}(\vec{r}, t) = 0 , \tag{94}$$

where

$$J_{Ei}(\vec{r}, t) = \sum_{\vec{q}} \omega(\vec{q}) V_i f(\vec{q}, \vec{r}, t) ,$$
$$J_{Qij}(\vec{r}, t) = \sum_{\vec{q}} q_i V_j f(\vec{q}, \vec{r}, t) , \tag{95}$$

representing energy current and quasimomentum flux. To derive hydrodynamic equations for the conservation laws (18) and (19), one has to solve the Peierls equations. This is a difficult task.[10,14] Here, we follow Beck[10] and use the mean free time approximation. The collision operator $C[f]$ [Eq. (90)] is replaced by the approximation

$$C[f] = -(f - f^d_{\mathrm{LE}})/\tau_N(\vec{q}) - (f - f^d_{\mathrm{LE}})/\tau_U(\vec{q}) , \tag{96}$$

f^d_{LE} being the drifting-local-equilibrium distribution function. In the classical limit, it is given by

$$f^d_{\mathrm{LE}}(\vec{q}, \vec{r}, t) = \frac{1}{\beta(\vec{r}, t)[\omega(\vec{q}) - \vec{q} \cdot \vec{U}(\vec{r}, t)]} ,$$
$$\beta(\vec{r}, t) = 1/k_B T(\vec{r}, t) , \tag{97}$$

$\vec{U}$ denoting the drift velocity of the phonon gas; f_{LE} satisfies $C[f_{\mathrm{LE}}] = 0$; τ_N is the relaxation time for normal, and τ_U for umklapp processes.

The next step is to assume that the deviation δf of f from equilibrium f_0 is small, allowing for linearization of the equations involving f. This excludes the description of nonlinear heat-pulse progagation. Let us therefore expand

$$f(\vec{q}, \vec{r}, t) = f_0(\vec{q}) + m(\vec{q}) g(\vec{q}, \vec{r}, t)$$
$$f_{\mathrm{LE}}(\vec{q}, \vec{r}, t) \approx f_0(\vec{q}) - m(\vec{q}) \omega(\vec{q}) \delta\beta(\vec{r}, t)/\beta_0 \tag{98}$$
$$f^d_{\mathrm{LE}}(\vec{q}, \vec{r}, t) \approx f_0(\vec{q}) - m(\vec{q})[\omega(\vec{q}) \delta\beta(\vec{r}, t)/\beta_0 - \vec{U}(\vec{r}, t)\vec{q}]$$

with

$$m(\vec{q}) = -1/\beta_0 \omega^2(\vec{q}) , \tag{99}$$

$$f_0(\vec{q}) = 1/\beta_0 \omega(\vec{q}) . \tag{100}$$

After substitution of Eqs. (96), (97), and (98) into the Peierls-Boltzmann equation, the equation for

the unknown g reads

$$\left(\frac{\partial}{\partial t}+\vec{V}\,\frac{\partial}{\partial \vec{r}}+\tau^{-1}\right)g=-\frac{\omega(\vec{q})}{\tau}\,\frac{\delta\beta}{\beta_0}+\frac{1}{\tau_N}\,\vec{U}\cdot\vec{q} \tag{101}$$

with

$$[\tau(\vec{q})]^{-1}=[\tau_N(\vec{q})]^{-1}+[\tau_R(\vec{q})]^{-1}. \tag{102}$$

Upon Fourier transforming all quantities according to

$$f(\vec{q},\vec{r},t)=\sum_{\vec{q}'}e^{i\vec{q}'\cdot\vec{r}}\int_{-\infty}^{+\infty}d\omega\, e^{-i\omega t}f(\vec{q},\vec{q}',\omega), \tag{103}$$

the solution of (101) is formally given by

$$g(\vec{q},\vec{q}',\omega)=\{-i\omega+i\vec{q}'\cdot\vec{V}(\vec{q})+[\tau(\vec{q})]^{-1}\}^{-1}\times\left(-\frac{\omega(\vec{q})}{\tau(\vec{q})}\,\frac{\delta\beta(\vec{q}',\omega)}{\beta_0}+\frac{1}{\tau_N(\vec{q})}\,\vec{U}(\vec{q}',\omega)\cdot\vec{q}\right). \tag{104}$$

Thus g depends on two unknown functions $\delta\beta$ and $\vec{U}$. For a cubic system, $\vec{U}$ may be eliminated with the aid of the conservation laws for energy [Eq. (93)] and quasimomentum [Eq. (104]. This leads to a hydrodynamic equation for $\delta\beta$, giving the dispersion law

$$\omega^2+i\omega(\langle\tau_U^{-1}\rangle+q^2C_S^2\langle\tau_N\rangle)-q^2C_S^2=0, \tag{105}$$

where

$$C_S^2=\frac{1}{3}\left(\frac{1}{N}\sum_{\vec{q}'}\frac{\partial\omega_0}{\partial\vec{q}'}\,\vec{q}'\,\frac{1}{\omega_0(\vec{q}')}\right)^2\Big/\left(\frac{1}{N}\sum_{\vec{q}'}\frac{\vec{q}'^2}{\omega_0^2(\vec{q}')}\right), \tag{106}$$

$$\langle\tau_U^{-1}\rangle=\left(\frac{1}{N}\sum_{\vec{q}'}\frac{\vec{q}'^2}{\omega_0^2(\vec{q}')\tau_U(\vec{q}')}\right)\Big/\left(\frac{1}{N}\sum_{\vec{q}'}\frac{\vec{q}'^2}{\omega_0^2(\vec{q}')}\right), \tag{107}$$

$$\langle\tau_N\rangle=\left[5\left(\frac{1}{N}\sum_{\vec{q}'}\frac{1}{\omega_0(\vec{q}')}\,\vec{q}'\,\frac{\partial\omega}{\partial\vec{q}'}\right)^2\right]^{-1}\times\left[5\,\frac{1}{N}\sum_{\vec{q}'}\left(\frac{\partial\omega_0}{\partial\vec{q}'}\right)^2\tau_N\,\frac{1}{N}\sum_{\vec{q}'}\frac{1}{\omega_0^2}\,\vec{q}'^2+\frac{1}{N}\sum_{\vec{q}'}\frac{1}{\omega_0^2(\vec{q}')}\,\vec{q}'^2\left(\frac{\partial\omega_0}{\partial\vec{q}'}\right)^2\tau_N+2\,\frac{1}{N}\sum_{\vec{q}'}\frac{1}{\omega_0^2(\vec{q}')}\left(\vec{q}'\cdot\frac{\partial\omega_0}{\partial\vec{q}'}\right)^2\tau_N-10\,\frac{1}{N}\sum_{\vec{q}'}\frac{1}{\omega_0(\vec{q}')}\,\vec{q}'\cdot\frac{\partial\omega_0}{\partial\vec{q}'}\,\tau_N\,\frac{1}{N}\sum_{\vec{q}'}\frac{1}{\omega_0(\vec{q}')}\,\vec{q}'\cdot\frac{\partial\omega_0}{\partial\vec{q}'}\right]. \tag{108}$$

The expression (106) for the second-sound velocity, which was first given in this general form by Kwok,[17] agrees with our expression (79), derived from the Green's-function approach. The susceptibility associated with the dispersion law (105) is given by

$$\chi_{\beta\beta}(\vec{q},\omega)=-\frac{1}{\omega^2+i\omega(\langle\tau_U^{-1}\rangle+\vec{q}^2C_S^2\langle\tau_N\rangle)-\vec{q}^2C_S^2}, \tag{109}$$

so that

$$\hat{S}_{\beta\beta}(\vec{q},\omega)=-\frac{\chi''_{\beta\beta}(\vec{q},\omega)}{\omega\chi_{\beta\beta}(\vec{q},0)}=\frac{2\omega_S^2\,\Gamma(\vec{q})}{(\omega^2-\omega_S^2)^2+\omega^2\Gamma^2(\vec{q})}, \tag{110}$$

where

$$\omega_S^2=\vec{q}^2C_S^2,\quad \Gamma(\vec{q})=\langle\tau_U^{-1}\rangle+\omega_S^2\langle\tau_N\rangle. \tag{111}$$

Expression (110) is certainly an approximation because only the real part of the memory function is taken into account. In fact, the exact expression may be obtained from Eq. (86) by considering $\mathcal{H}(\vec{q})$ and $\dot{\mathcal{H}}(\vec{q})$ as dynamic variables. The result is

$$\hat{S}_{\beta\beta}(\vec{q},\omega)=\frac{2\Sigma'(-i\omega,\vec{q})\omega_S^2}{[\omega^2-\omega_S^2-\omega\Sigma''(-i\omega,\vec{q})]^2+[\omega\Sigma'(-i\omega,\vec{q})]^2}, \tag{112}$$

where

$$\omega_S^2=\frac{\langle\dot{\mathcal{H}}(\vec{q})\,|\,\dot{\mathcal{H}}(\vec{q})\rangle}{\langle\mathcal{H}(\vec{q})|\mathcal{H}(\vec{q})\rangle}.$$

$$\Sigma(\vec{q},z=-i\omega)=\langle\ddot{\mathcal{H}}(\vec{q})\Big|Q\,\frac{1}{z+iQLQ}\,Q\Big|\ddot{\mathcal{H}}(\vec{q})\rangle\Big/\langle\dot{\mathcal{H}}(\vec{q})\,|\,\dot{\mathcal{H}}(\vec{q})\rangle. \tag{113}$$

According to Eq. (86), this expression for ω_S^2 agrees with the Kwok expression (106) in the continuum limit. Comparing the spectral densities (110) and (112), it is seen that, in the dynamic approach, the imaginary part of the memory function is neglected. Expression (100) of the hydrodynamic approach is obtained from Eqs. (112) and (113) by assuming $\Sigma(z)=\Sigma(z=0)=\Gamma$.

The solutions of the dispersion law (105) are

$$\omega = \pm\omega_S\left[1 - \frac{1}{4}\left(\frac{\langle\tau_U^{-1}\rangle}{\omega_S} + \omega_S\langle\tau_N\rangle\right)^2\right]^{1/2} - \frac{i}{2}\left(\langle\tau_U^{-1}\rangle + \omega_S^2\langle\tau_N\rangle\right), \tag{114}$$

revealing that well-defined second sound requires many normal processes:

$$\omega\langle\tau_N\rangle \ll 1, \tag{115}$$

and umklapp processes should be rare,

$$\omega \gg \langle\tau_U^{-1}\rangle. \tag{116}$$

The combination of these two inequalities is the well-known window condition[18]

$$\langle\tau_N^{-1}\rangle \gg \omega \gg \langle\tau_U^{-1}\rangle, \tag{117}$$

defining the frequencies where second sound is expected to occur.

An estimate for the temperature dependence of $\langle\tau_N^{-1}\rangle$ and $\langle\tau_U^{-1}\rangle$ may be obtained from the memory function evaluated by anharmonic perturbation theory and expressions (99) and (100). For model I and sufficiently low temperatures, where the third-order term dominates, we obtain from Eqs. (59), (107), and (108),

$$\langle\tau_N\rangle = \alpha_I/T, \quad \langle\tau_U^{-1}\rangle = \beta_I T. \tag{118}$$

For model II, where only quartic anharmonicity is present, we find with the aid of Eq. (53),

$$\langle\tau_N\rangle = \alpha_{II}/T^2, \quad \langle\tau_U^{-1}\rangle = \beta_{II} T^2. \tag{119}$$

In both equations, $\langle\tau_U^{-1}\rangle$ increases with T, so that inequality (116) will be reversed at some T,

$$\omega \ll \langle\tau_U^{-1}\rangle. \tag{120}$$

In this case, the solution of the dispersion law (105) is

$$\omega \approx -i\omega_S^2\langle\tau_U^{-1}\rangle^{-1}, \tag{121}$$

corresponding to heat diffusion, instead of propagating second sound.

III. MOLECULAR-DYNAMICS RESULTS

In this section, we briefly sketch our molecular-dynamics technique and discuss some of the numerical results.

A. Molecular-dynamics technique

In the conventional molecular-dynamics technique,[19,20] one solves the set of coupled Newton's equations associated with a given Hamiltonian according to a set of difference equations with a time increment. This set of difference equations approximates Newton's equations. Starting from given initial conditions for the positions and velocities, the particles are then allowed to move, and the time evolution of their canonical variables $(X_l, \dot{X}_l)$ are calculated. Assuming the system is ergodic, estimates for microcanonical ensemble averages may be obtained in terms of time averages.

It would be preferable to have a molecular-dynamics technique, simulating a canonical ensemble, as most experiments are performed at constant global temperature. This was achieved by considering, in place of the Newton's equations, the coupled set of Langevin equations[8]

$$M\ddot{X}_l = -\frac{\partial\mathcal{H}}{\partial X_l} - \Gamma M\dot{X}_l + \eta_l(t), \tag{122}$$

where

$$\langle\eta_l(t)\eta_{l'}(t')\rangle = 2M\Gamma k_B T\delta(t-t')\delta_{ll'}. \tag{123}$$

Here, it is assumed that the particles suffer collisions with much lighter ones which represent the heat bath defining the temperature T. The collisions are described by the friction $\Gamma M\dot{X}_l$ and a random force $\eta_l(t)$. It may be shown that the stationary solution of the associated Fokker-Planck equation is the canonical distribution function

$$P_{\text{eq}}(\dot{X}_1, \ldots, \dot{X}_N, X_1, \ldots, X_N) = \exp(-\mathcal{H}/k_B T). \tag{124}$$

Starting from initial values for positions and velocities, the particles are then allowed to move under the influence of the computer-generated random force. The temporal evolution of the variables are then calculated with a set of difference equations approximating the Langevin equations (122). On this basis, one obtains

$$X_l(t),\ \dot{X}_l(t),\ \ddot{X}_l(t),\ \text{etc.} \tag{125}$$

For a detailed description of the algorithm and the random force generation, we refer to Ref. 8. The system is then allowed to age or, in other words, to reach equilibrium. After this interval, the subsequent 10^5 steps are used to perform time averages representing canonical ensemble averages.

From the Langevin equations (122), it is obvious that the dynamic properties will be modified, in particular, owing to the damping term. To reduce this modification, Γ must be chosen in such a way that

$$1/\Gamma \gg \tau_c, \tag{126}$$

where τ_c denotes the characteristic time of the dynamics. This guarantees that the excitations do not become overdamped owing to the friction term. Another important constraint on Γ evolves from the energy conservation of a Hamiltonian system. Since our system evolves according to the Langevin equation, it follows that

$$\frac{d\mathcal{H}}{dt} = \sum_l \frac{\partial \mathcal{H}}{\partial M\dot{X}_l} M\ddot{X}_l + \frac{\partial \mathcal{H}}{\partial X_l}\dot{X}_l$$

$$= -\sum_l [\Gamma M\dot{X}_l^2 - \dot{X}_l \eta_l(t)] . \quad (127)$$

Consequently, energy is not conserved because the Hamiltonian system is in contact with the heat bath. To avoid artifical features due to the random noise pulses, the mean time between two pulses must be small compared to τ_c. In this case, we may average Eq. (127) over some pulses. This leads to

$$\frac{d\mathcal{H}}{dt} = -\Gamma[2E_{\rm kin}(t) - Nk_BT] = -\delta E_k(t) . \quad (128)$$

With the ansatz

$$\delta E_k(t) = \alpha e^{-t/\tau} \quad (129)$$

and

$$\frac{dH}{dt} = \frac{dH}{d\delta E_k}\frac{d\delta E_k}{dt} = \frac{dH}{dT}\frac{dT}{d\delta E_k}\frac{d\delta E_k}{dt} \approx \frac{2C_v}{k_B}\frac{d\delta E_k}{dt} , \quad (130)$$

we find

$$\tau = (C_v/k_B)(1/\Gamma) , \quad (131)$$

where C_v is the specific heat. Accordingly, energy is nearly conserved within the characteristic time τ_c, provided that

$$\tau = (C_v/k_B)(1/\Gamma) \gg \tau_c . \quad (132)$$

Moreover, owing to the fact that the system evolves according to the Langevin equation, the time interval $\tau_{\rm ch}$ over which an evolution is followed must be larger than τ so that

$$\tau \ll \tau_{\rm ch} . \quad (133)$$

Combining inequalities (132) and (133), we finally obtain

$$\tau_{\rm ch} \gg C_v/k_B\Gamma \gg \tau_c . \quad (134)$$

From this relation, it becomes evident that energy can be nearly conserved provided Γ and the chain length $\tau_{\rm ch}$ are appropriately chosen. An exception is very close to T_c, where the characteristic time τ_c becomes very long.

In the calculations presented here, we have considered systems of 8000 particles defined by Hamiltonian (1) and model parameters specified in Eqs. (2) and (3). The systems were subjected to periodic boundary conditions. In the time interval, where time averages have been performed, Γ was chosen as

$$\Gamma = 0.005 . \quad (135)$$

B. Numerical results

Let us now turn to the discussion of the numerical results as obtained by means of the molecular-dynamics technique sketched above. To investigate the excitation spectrum, we calculated the spectral densities

$$\hat{S}_{XX}(\vec{q}, \omega) = \frac{\int_{-\infty}^{+\infty} dt\, e^{-i\omega t}\langle X(-\vec{q}, t) X(\vec{q}, 0)\rangle}{\langle X(-\vec{q}, 0) X(\vec{q}, 0)\rangle} , \quad (136)$$

and

$$\hat{S}_{\mathcal{H}\mathcal{H}}(\vec{q}, \omega) = \frac{\int_{-\infty}^{+\infty} dt\, e^{-i\omega t}\langle \mathcal{H}(-\vec{q}, t)\mathcal{H}(\vec{q}, 0)\rangle}{\langle \mathcal{H}(-\vec{q}, 0)\mathcal{H}(\vec{q}, 0)\rangle} , \quad (137)$$

where the variables $X(\vec{q})$ and $\mathcal{H}(\vec{q})$ are defined in Eqs. (7) and (8). The Green's functions introduced in Sec. II B are related to the spectral densities as follows:

$$G_{AA}^{\dagger}(z) = \lim_{\epsilon \to 0^+} G_{AA}^{\dagger}(z = -i\omega + \epsilon) = -\chi_{AA}(\omega) , \quad (138)$$

where in the classical limit,

$$\chi''_{AA}(\omega) = \pi\beta\omega S_{AA}(\omega) . \quad (139)$$

Next we present and discuss the numerical results as obtained for model I [Eq. (2)], exhibiting a ferrodistortive phase below $T = T_c \approx 7.1$. For $T < T_c$, order-parameter and energy fluctuations are coupled and second sound is expected to occur in both $\hat{S}_{XX}(\vec{q}, \omega)$ and $\hat{S}_{\mathcal{H}\mathcal{H}}(\vec{q}, \omega)$ [see Sec. II D]. At high frequencies and low temperatures we find, as expected, that the spectrum of $\hat{S}_{XX}(\vec{q}, \omega)$ is dominated by the phonon resonance of the optic branch. Figure 1 shows the dispersion law of the optical branch as determined from the position of the peak maxima for $k_BT = 0.25$. For comparison, we included the bare phonon frequency, calculated from Eq. (52). The excellent agreement reveals that at

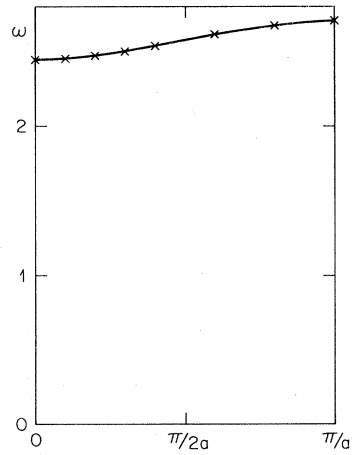

FIG. 1. Phonon dispersion law at $k_BT = 0.125$. The full line represents the bare phonon frequency as obtained from Eq. (52) with $\langle X^2\rangle$ taken from the molecular-dynamics estimate (Table I). The crosses correspond to the positions of the peak maxima in $\hat{S}_{XX}(\vec{q}, \omega)$ for $\vec{q} = (q_1, 0, 0)$.

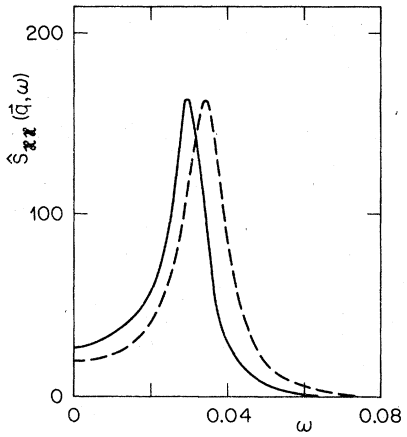

FIG. 2. $\hat{S}_{\mathcal{H}\mathcal{H}}(\vec{q},\omega)$ of model I at $k_BT=0.125$ for $\vec{q}=(\pi/10a,0,0)$. Solid line, molecular-dynamics results; dashed line, fit to Eq. (110).

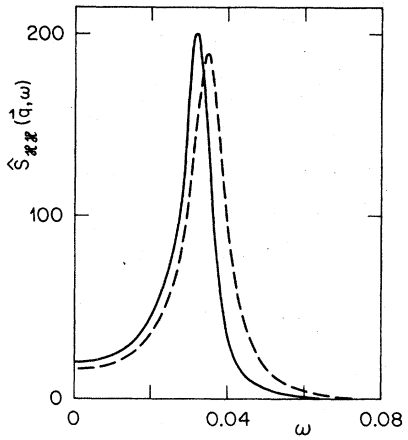

FIG. 4. $\hat{S}_{\mathcal{H}\mathcal{H}}(\vec{q},\omega)$ of model I at $k_BT=0.5$ for $\vec{q}=(\pi/10a,0,0)$. Solid line, molecular-dynamics results; dashed line, fit to Eq. (110).

sufficiently low temperatures and high frequencies, perturbation theory works very well.

At low frequencies, this will no longer be the case due to the singularity expressing energy conservation. In fact, here we expect in both $\hat{S}_{XX}(\vec{q},\omega)$ and $\hat{S}_{\mathcal{H}\mathcal{H}}(\vec{q},\omega)$ an additional low-frequency resonance corresponding to second sound or heat diffusion. This expectation is confirmed by the numerical results shown in Figs. 2–5. Here, we plotted the low-frequency part of $\hat{S}_{\mathcal{H}\mathcal{H}}(\vec{q},\omega)$ at $\vec{q}=(\pi/10a,0,0)$ for various temperatures, revealing a well-defined resonance. The damping is seen to increase, however, for $T\neq T\approx 0.125$ indicating the existence of a window condition. To study this point more quantitatively, we also fitted the expression for $\hat{S}_{\beta\beta}(\vec{q},\omega)$ [Eq. (110)] predicted by the hydrodynamic approach to the molecular-dynamics results. In this fit, $\omega_S^2=C_S^2q^2$ has been calculated from Eq. (106), using for ω_0 expression (52), where $\langle X^2\rangle$ has been taken from the molecular-dynamics data (see Table I). The parameters α_I and β_I in the damping constant Γ [Eqs. (111) and (118)] were determined by means of a least-square fit to the peak height of the numerically determined $\hat{S}_{\mathcal{H}\mathcal{H}}(\vec{q},\omega)$ for $k_BT=0.125$, 0.25, 0.5, and 1, yielding

$$\alpha_I=1.042\pm0.070,\quad \beta_I=0.0167\pm0.0007. \tag{140}$$

In Figs. 2–5, we compare the resulting spectral densities with the molecular-dynamics results. The temperature dependence of the damping constant [Eq. (101)]

$$\Gamma_I=\beta_I T+\omega_S^2\alpha_I/T=\langle\tau_U^{-1}\rangle+\omega_S^2\langle\tau_N\rangle \tag{141}$$

as obtained from the estimated values for α_I and β_I [Eq. (140)] is compared in Fig. 6 with the effective damping constant Γ_{eff} as determined by the

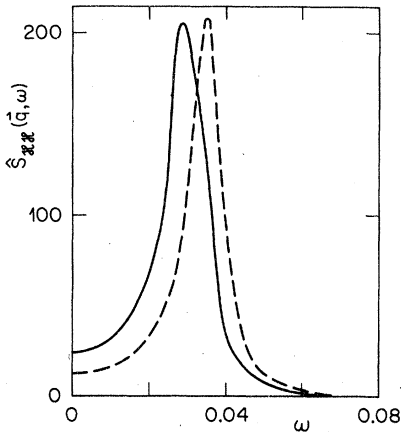

FIG. 3. $\hat{S}_{\mathcal{H}\mathcal{H}}(\vec{q},\omega)$ of model I at $k_BT=0.25$ for $\vec{q}=(\pi/10a,0,0)$. Solid line, molecular-dynamics results; dashed line, fit to Eq. (110).

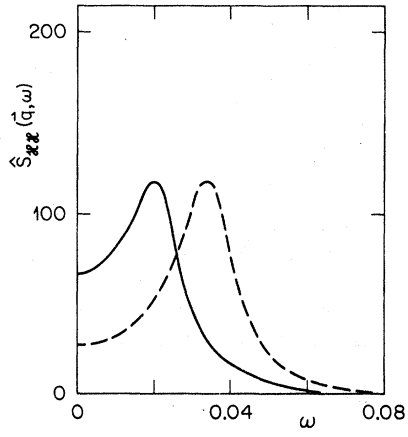

FIG. 5. $\hat{S}_{\mathcal{H}\mathcal{H}}(\vec{q},\omega)$ of model I at $k_BT=1$ for $\vec{q}=(\pi/10a,0,0)$. Solid line, molecular-dynamics results; dashed line, fit to Eq. (110).

TABLE I. Numerical estimates for $\omega_S = C_S q$ [Eq. (106)], $\langle X^2 \rangle$, $\omega_{S\,\mathrm{eff}}$, Γ_{eff}, and Γ_{fit} [Eq. (141)] for $\vec{q} = (\pi/10a, 0, 0)$ in model I. $\omega_{S\,\mathrm{eff}}$ and Γ_{eff} are determined by the peak height and position of the numerical data by assuming Eq. (110).

$k_B T$	ω_S	$\langle X^2 \rangle$	$\omega_{S\,\mathrm{eff}}$	Γ_{eff}	Γ_{fit}
0.125	0.036	8.988	0.031	0.013	0.013
0.25	0.036	8.936	0.029	0.010	0.010
0.50	0.036	8.869	0.033	0.010	0.011
1	0.036	8.733	0.025	0.021	0.018
1.3	0.037	8.643	0.024	0.026	0.023
1.6	0.037	8.552	0.024	0.031	0.028
2	0.037	8.421	0.022	0.039	0.034

peak position and height by assuming Eq. (110). The resulting $\omega_{S\,\mathrm{eff}}$ and Γ_{eff} are listed in Table I. The temperature dependence of Γ and Γ_{eff} nicely confirms the existence of the window condition predicted by the hydrodynamic approach. In fact, $\Gamma(T)$ has a minimum around $k_B T = 0.28$ and increases for T below and above this temperature. From Table I, it can be seen, however, that $\Gamma_{\mathrm{eff}} - \Gamma_{\mathrm{fit}}$ increases with T. This may be understood in terms of the next higher-order contribution to the relaxation times giving rise to a T^2 term for the umklapp processes. The same effect also partially explains the mismatch of the peak maxima with increasing temperature (see Figs. 2–5). Table I reveals, however, that also the difference between the "bare" second-sound frequency ω_S and the effective one increases with T. This systematic discrepancy cannot be attributed to the shift of the phonon frequency ω_0 entering Eq. (75), due to the cubic and quartic anharmonicity. In fact, in the temperature range $k_B T < 2$ deviations between ω_0, defined by Eq. (52) and the actual position of the phonon peaks in $\hat{S}_{XX}(\vec{q}, \omega)$ are extremely small (see also Fig. 1). Accordingly, we must conclude the actual second-sound frequency is overestimated, and does not treat its temperature dependence correctly, because the imaginary part of the memory function is neglected [see Eq. (112)].

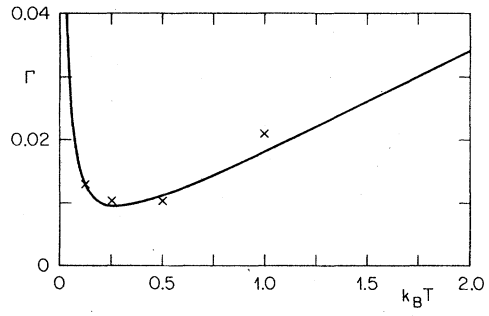

FIG. 6. Temperature dependence of the damping constant Γ for model I. Solid line, according to Eqs. (111), (118), and (140); ×, effective damping constant determined by the peak position and height of the numerical $\hat{S}_{\mathcal{H}\mathcal{H}}(\vec{q}, \omega)$.

Nevertheless, this comparison reveals that the agreement between the predictions of the hydrodynamic approach and the molecular-dynamics results is quite good. In particular, the most crucial prediction, namely, that well-defined second sound will occur only in a temperature window, is quantitatively confirmed, even in a regime where the validity of hydrodynamics is no longer guaranteed. Above the temperature where Γ reaches its minimum, second sound becomes increasingly damped and finally goes over to heat diffusion, as illustrated in Fig. 7.

An interesting feature of model I, which we have not yet considered, is the coupling between the order-parameter and energy fluctuations below $k_B T = k_B T_c \approx 7.1$. Owing to this coupling [see Sec. II D], second sound and the phonon resonance will appear in both $\hat{S}_{XX}(\vec{q}, \omega)$ and $\hat{S}_{\mathcal{H}\mathcal{H}}(\vec{q}, \omega)$. According to Eqs. (88) and (89), the strength of the second-sound peak in $\hat{S}_{XX}$ and of the phonon resonance in $\hat{S}_{\mathcal{H}\mathcal{H}}$ will be rather small, however. To substantiate this expectation, we refer to the ratio of the peak heights for $k_B T = 0.125$ in $\hat{S}_{XX}(\vec{q}, \omega)$,

$$\hat{S}_{XX}(\vec{q}, \omega_S)/\hat{S}_{XX}(\vec{q}, \omega_0) \approx 1 \times 10^{-3}, \tag{142}$$

for $\vec{q} = (\pi/10a, 0, 0)$, as obtained from molecular dynamics. These results can be compared with the predictions of the four-variable theory [Eqs. (85) and (88)] yielding for $\omega_S \approx 0.030$, $\omega_0 \approx 2.42$, $k_B T = 0.125$,

$$R^-_{XX}/R^+_{XX} \approx 0.3 \times 10^{-3}, \tag{143}$$

which is in reasonable agreement with the above numerical result.

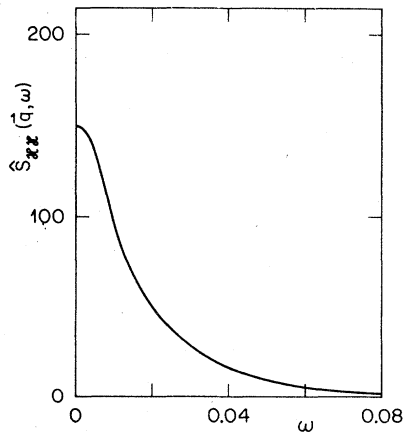

FIG. 7. $\hat{S}_{\mathcal{H}\mathcal{H}}(\vec{q}, \omega)$ of model I at $k_B T = 2$ for $\vec{q} = (\pi/10a, 0, 0)$ as obtained from molecular dynamics.

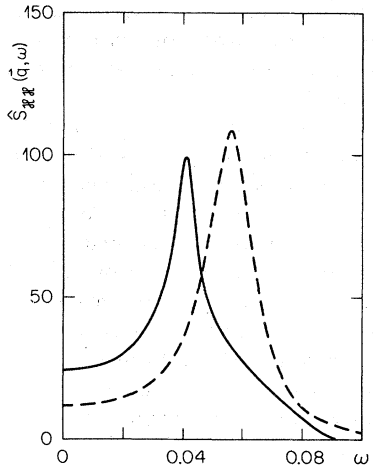

FIG. 8. $\hat{S}_{\mathcal{H}\mathcal{H}}(\vec{q},\omega)$ of model II at $k_BT=0.75$ for $\vec{q}=(\pi/10a,0,0)$. Solid line, molecular-dynamics results; dashed line, fit to Eq. (110).

In model II, which does not exhibit an ordered phase [Eq. (3)], energy and displacement fluctuations are no longer coupled and only quartic anharmonicity is present. As a consequence (see Sec. II D), second sound occurs only in $\hat{S}_{\mathcal{H}\mathcal{H}}(\vec{q},\omega)$. The interest in this model stems from the fact that the relaxation times for umklapp and normal processes will have, at low temperature, a quadratic temperature dependence [Eq. (119)]. Moreover, due to the absence of a coupling between energy and displacement fluctuations, second sound or heat diffusion will occur only in $\hat{S}_{\mathcal{H}\mathcal{H}}(\vec{q},\omega)$. Accordingly, two variable theories should be sufficient to describe the excitation spectrum. In particular, $\mathcal{H}(\vec{q})$ and the field momentum density $\vec{\mathbf{Q}}(\vec{q})$ are sufficient to describe the low-frequency and small wave-vector regime of $\hat{S}_{\mathcal{H}\mathcal{H}}(\vec{q},\omega)$. These are essentially the assumptions of the hydrodynamic approach outlined in Sec. II C, where the coupling of energy or quasimomentum to other variables is not considered. In principle, therefore, a comparison between the molecular-dynamics results for model II and the predictions of the hydrodynamic approach is not affected by the coupling to the order-parameter fluctuations.

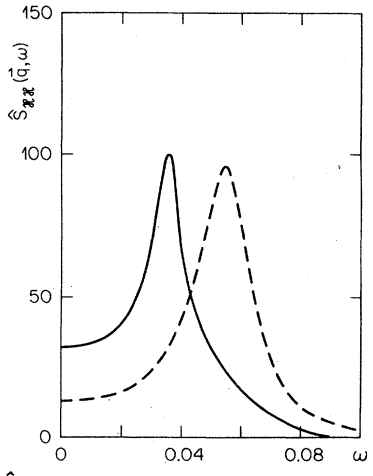

FIG. 9. $\hat{S}_{\mathcal{H}\mathcal{H}}(\vec{q},\omega)$ of model II at $k_BT=1$ for $\vec{q}=(\pi/10a,0,0)$. Solid line, molecular-dynamics results; dashed line, fit to Eq. (110).

TABLE II. Numerical estimates for $\omega_S = C_S q$ [Eq. (106)], $\langle X^2\rangle$, $\omega_{S\,\mathrm{eff}}$, Γ_{eff}, and Γ_{fit} [Eq. (145)] for $\vec{q}=(\pi/10a,0,0)$ in model II. $\omega_{S\,\mathrm{eff}}$ and Γ_{eff} are determined by the peak position and height of the numerical data by assuming Eq. (110).

k_BT	ω_S	$\langle X^2\rangle$	$\omega_{S\,\mathrm{eff}}$	Γ_{eff}	Γ_{fit}
0.5	0.059	0.170	0.043	0.028	0.027
0.75	0.058	0.250	0.045	0.022	0.019
1	0.057	0.342	0.039	0.022	0.022
1.5	0.056	0.463	0.033	0.036	0.039

Figures 8 and 9 show the calculated frequency dependence of $\hat{S}_{\mathcal{H}\mathcal{H}}(\vec{q},\omega)$ at $k_BT=0.75$ and 1, respectively, for model II. For comparison, we also fitted the expression for $\hat{S}_{\beta\beta}(\vec{q},\omega)$ [Eq. (110)], predicted by the hydrodynamic approach to the molecular-dynamics results. In this fit, $\omega_S^2=C_S^2q^2$ was calculated from Eq. (106), using for ω_0 expression (52), invoking the numerical value for $\langle X^2\rangle$, listed in Table II. The parameters α_{II} and β_{II} in the damping constant Γ [Eqs. (111) and (118)] were determined by means of a least-square fit to the peak height of the numerically determined $\hat{S}_{\mathcal{H}\mathcal{H}}(\vec{q},\omega)$ for $k_BT=0.5$, 0.75, and 1, yielding

$$\alpha_{\mathrm{II}}=1.63\pm0.19,\quad \beta_{\mathrm{II}}=0.0094\pm0.0022\,. \tag{144}$$

The temperature dependence of the damping con-

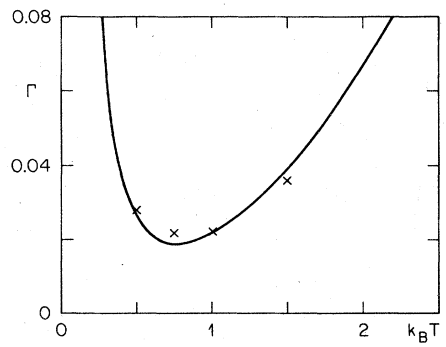

FIG. 10. Temperature dependence of the damping constant Γ for model II. Solid line, according to Eqs. (111), (119), and (144); ×, effective damping constant determined by the peak position and height of the numerical $\hat{S}_{\mathcal{H}\mathcal{H}}(\vec{q},\omega)$.

stant [Eq. (113)],

$$\Gamma_{II} = \beta_{II} T^2 + \omega_S^2 \alpha_{II}/T^2 = \langle \tau_U^{-1} \rangle + \omega_S^2 \langle \tau_N \rangle \qquad (145)$$

with the above values for α_{II} and β_{II} and the ω_S listed in Table II is shown in Fig. 10. For comparison, we included the effective damping constant Γ_{eff} as determined by the peak position and height by assuming Eq. (110). The resulting $\omega_{S\,eff}$ and Γ_{eff} are given in Table II. The temperature dependence of Γ and Γ_{eff} (Fig. 10) again confirms nicely the existence of the window condition predicted by the hydrodynamic approach. This is also illustrated by the well-defined second-sound peaks in Figs. 8 and 9. In contrast to model I, there is no systematic discrepancy between Γ_{fit} and Γ_{eff}. Table II reveals, however, that as in model I ω_S given by Eqs. (106) and (111) overestimates the actual second-sound frequency $\omega_{S\,eff}$ and does not account for the temperature dependence. This discrepancy must again be attributed to neglect of the imaginary part of the memory function [see Eq. (112)] in the hydrodynamic approach. Nevertheless, the overall agreement between the molecular-dynamics results and the predictions of the hydrodynamic treatment is again quite good.

It should be emphasized that the values of the model parameters in models I and II [Eqs. (2) and (3)] do not represent a particular choice in the sense that the occurrence of second sound is more likely. Apart from the sign of A, we have chosen them more or less at random. This then demonstrates that well-defined second sound should be a rather usual low-temperature phenomenon provided the system is sufficiently clean.

[1] C. C. Ackerman, B. Bertman, H. A. Fairbank, and R. A. Guyer, Phys. Rev. Lett. 16, 789 (1966).
[2] C. C. Ackerman and W. C. Overton, Phys. Rev. Lett. 22, 764 (1969).
[3] T. F. McNelly, S. J. Rogers, P. J. Channin, R. J. Rollefson, W. M. Goubau, G. E. Schmidt, J. A. Krumhansl, and R. O. Pohl, Phys. Rev. Lett. 24, 100 (1970).
[4] V. Narayanamurti and R. C. Dynes, Phys. Rev. Lett. 28, 1461 (1972).
[5] D. Pohl and V. Irniger, Phys. Rev. Lett. 36, 480 (1976).
[6] D. H. Tsai and R. A. MacDonald, Phys. Rev. B 14, 4714 (1976).
[7] T. Schneider, E. Stoll, and Y. Hiwatari, Phys. Rev. Lett. 39, 1382 (1977).
[8] T. Schneider and E. Stoll, Phys. Rev. B 17, 1302 (1978).
[9] C. P. Enz, Rev. Mod. Phys. 46, 705 (1974).
[10] H. Beck, in *Dynamical Properties of Solids*, edited by G. K. Horton and A. A. Maradudin (North-Holland, Amsterdam, 1974), Vol. II, p. 205.
[11] A. D. Bruce, Ferroelectrics 12, 21 (1976).
[12] H. Mori, Prog. Theor. Phys. 33, 423 (1965); 34, 399 (1965).
[13] P. F. Meier, Phys. Kondens. Mater. 17, 17 (1973).
[14] J. A. Süssman and A. Thellung, Proc. R. Soc. London 81, 1122 (1963).
[15] T. Schneider and E. Stoll, Phys. Rev. B 13, 1216 (1976).
[16] S. Sarbach, Phys. Rev. B 15, 2694 (1977).
[17] P. C. Kwok, Physics 3, 221 (1967).
[18] J. A. Krumhansl, Proc. Phys. Soc. 85, 921 (1965).
[19] A. Rahman, Phys. Rev. 136, A405 (1964).
[20] L. Verlet, Phys. Rev. 159, 98 (1967).